Eur Biophys J (2000) 29: 398–408

ARTICLE

Olivier Thoumine · Pierre Kocian · Arlette Kottelat
Jean-Jacques Meister

Short-term binding of fibroblasts to fibronectin: optical tweezers experiments and probabilistic analysis

Received: 2 November 1999 / Revised version: 6 March 2000 / Accepted: 19 April 2000

Abstract The biophysical properties of the interaction between fibronectin and its membrane receptor were inferred from adhesion tests on living cells. Individual fibroblasts were maintained on fibronectin-coated glass for short time periods (1–16 s) using optical tweezers. After contact, the trap was removed quickly, leading to either adhesion or detachment of the fibroblast. Through a stochastic analysis of bond kinetics, we derived equations of adhesion probability versus time, which fit the experimental data well and were used to compute association and dissociation rates ($k_+ = 0.3$–$1.4\ s^{-1}$ and $k_{off} = 0.05$–$0.25\ s^{-1}$, respectively). The bond distribution is binomial, with an average bond number ≤10 at these time scales. Increasing the fibronectin density (100–3000 molecules/μm^2) raised k_+ in a diffusion-dependent manner, leaving k_{off} relatively unchanged. Increasing the temperature (23–37 °C) raised both k_+ and k_{off}, allowing calculation of the activation energy of the chemical reaction (around 20 k_BT). Increasing the compressive force on the cell during contact (up to 60 pN) raised k_+ in a logarithmic manner, probably through an increase in the contact area, whereas k_{off} was unaffected. Finally, by varying the pulling force to detach the cell, we could distinguish between two adhesive regimes, one corresponding to one bond, the other to at least two bonds. This transition occurred at a force around 20 pN, interpreted as the strength of a single bond.

Key words Cell adhesion · Receptor-ligand interaction · Binomial bond distribution · Integrin

O. Thoumine · P. Kocian · A. Kottelat · J.-J. Meister (✉)
Biomedical Engineering Laboratory,
Swiss Federal Institute of Technology,
1015 Lausanne, Switzerland
e-mail: Jean-Jacques.Meister@epfl.ch

Introduction

Cell adhesion is essential to many phenomena in biology, such as rolling of leukocytes on the endothelium during inflammation (Springer 1994), or recognition of the extracellular matrix by the leading edge of migrating fibroblasts (Huttenlocher et al. 1995). One important step in these interactions is the formation of initial bonds, which allow close contact between the two surfaces (a few tens of nanometres) and subsequent strengthening of adhesion. At the molecular level, cell adhesion involves specific non-covalent binding of a transmembrane receptor to either a counter receptor on the surface of another cell or an extracellular protein ligand. The overall adhesion of a cell can essentially be described by the number of receptor-ligand complexes at a given time, which depends in particular on the quantity of available receptors and ligands, and on the affinity of the interaction. A large number of adhesion receptors have been described to date, which fall into four main categories: immunoglubulin-like, selectins, cadherins, and integrins. Their sequence, structure, and function are well described but their physicochemical properties are only beginning to be explored (Pierres et al. 1998a).

Adhesion usually occurs in the presence of a specific mechanical environment, e.g. blood flow on rolling leukocytes (Alon et al. 1995) or fibroblast traction on cell-matrix connections (Lauffenburger and Horwitz 1996). Thus, it is important to assess the physical characteristics of receptor-ligand binding. Adhesive interactions have been tested by several techniques (Pierres et al. 1998b), including atomic force microscopy (Hinterdorfer et al. 1996), optical force microscopy (Stout and Webb 1998), micropipet-based force transducers (Evans et al. 1991, 1995; Shao and Hochmuth 1996; Chesla et al. 1998), centrifugation (Lotz et al. 1989; Piper et al. 1998), and shear flow (Tha et al. 1986; Alon et al. 1995; Pierres et al. 1995a, b). Such studies have shown that the forces involved in receptor-ligand recognition, lying in the range of 1–100 pN, act on short

distances (around 0.1–1 nm). Thus, the binding pocket corresponds to a potential well on the order of several times the thermal energy (Evans et al. 1995; Wong et al. 1997).

From a biochemical perspective, one may describe the interaction between a receptor and its ligand as a reversible chemical reaction, characterized by association and dissociation rates, typically in the range of 0.01–10 s^{-1} (Kaplanski et al. 1993; Lauffenburger and Linderman 1993; Schmidt et al. 1994; Alon et al. 1995). These parameters depend on whether the molecules are in solution, free to diffuse in the plasma membrane (e.g. a receptor), or immobilized onto surfaces (e.g. an adsorbed ligand). For example, association should rely on two subsequent processes: the diffusion of the receptor in the vicinity of a ligand, followed by the reaction itself (Bell 1978). Moreover, the reaction rates are sensitive to the distance between interacting surfaces (Kaplanski et al. 1993; Pierres et al. 1997) and to the disruptive force applied on the bonds. Several mathematical expressions have been proposed to assess the influence of a pulling force on the dissociation rate (Bell 1978; Hammer and Lauffenburger 1987; Dembo et al. 1988; Evans et al. 1991; Evans and Ritchie 1997), some of which having been verified experimentally (Alon et al. 1995; Piper et al. 1998). However, the effects of compression and temperature on kinetic rates have not been addressed other than theoretically (Hammer and Lauffenburger 1987; Dembo et al. 1988). In addition, much recent work has focused on selectin-based interactions (Kaplanski et al. 1993; Alon et al. 1995; Piper et al. 1998), but little is known on the mechanics of molecular interactions with the extracellular matrix.

We focused here on the adhesion of fibroblasts to fibronectin, a well-characterized extracellular matrix protein able to interact, through an Arg-Gly-Asp sequence, with integrin receptors on the surface of many cell types (Ruoslahti 1988). The objective of this study was to measure the physicochemical properties of the fibronectin-integrin bond. Experiments with optical tweezers provided the fraction of adherent fibroblasts on a fibronectin-coated glass surface over time, under conditions of controlled fibronectin density, compressive and pulling forces, and temperature. The data were interpreted with a probabilistic analysis of bond kinetics, allowing computation of several parameters (association and dissociation rates, bond strength, and energy well).

Materials and methods

Cell culture

NIH mouse 3T3 fibroblasts were generously provided by C. Ruegg (ISREC, Epalinges, Switzerland). Cells were cultured in Dulbecco's modified Eagle's medium supplemented with 10% fetal bovine serum and 0.05% gentamycin. Cell culture reagents were purchased from Seromed (Germany).

Substrate treatment

Glass coverslips (50 m diameter, Polylabo, Geneva, CH) formed the bottom of 3-ml custom-made observation chambers. They were coated for 1 h at room temperature with bovine fibronectin (1 ml solutions of 0.3, 1, 3, or 10 μg/ml in PBS), and rinsed in PBS before use. Fibronectin was purchased commercially (Sigma, St. Louis, Mo., USA).

Determination of fibronectin density

Fibronectin from the same lot number was labeled with rhodamine at a fluorophore-to-protein ratio of 1:1 (coupling was done by Cytoskeleton, Denver, Colo., USA). Coverslips were coated with rhodamine-fibronectin, rinsed with PBS, then observed under an inverted microscope (Axiovert 135, Zeiss, Oberkochen, Germany) using a 63 × /1.25 oil objective and epifluorescence illumination. Light intensity was read with a photometer (MPM 100, Zeiss), set to maximum gain. The voltage readout was roughly proportional to the illuminated area (varied between 200 and 1200 μm^2 using diaphragms), and was taken as a measurement of fibronectin surface density. Light intensity (thus fibronectin density) increased linearly with initial fibronectin concentration (Table 1). Such linear dependence was reported by others (Codogno et al. 1987; Ingber 1990). To obtain absolute values, the amount of adsorbed fibronectin corresponding to a concentration of 10 μg/ml was determined by a conventional protein assay (Micro BCA, Pierce, Rockford, Ill., USA), using fibronectin as a standard. Absorbances at 562 nm were read with a spectrophotometer (Uvikon 930, Kontron Instruments). Both fibronectin present in the initial solution minus that in the bath after incubation, and the amount left behind on the substrate (harvested with 0.2% SDS in PBS) were quantified and averaged, giving 3.3 ± 0.8 μg for an area of 12.5 cm^2 ($n = 4$). The number of adsorbed molecules was obtained after dividing by the fibronectin molecular weight, i.e. 440,000 (Ruoslahti 1988). The densities for the lower concentrations were calculated by linear regression.

Set-up

The microscope is equipped with optical tweezers (PALM, Wolfratshausen, Germany), comprising a 1064 nm diode-pumped Nd:YAG solid-state laser (Laser Quantum, Manchester, UK) focused through a 100 × /1.4 oil objective (Ashkin et al. 1987), and a motorized 2D stage. The center of the trap was fixed at the focal point of the objective. The diode drive current, I, can be varied from 0 to 2.5 A. The laser power output, as measured with the photometer, is proportional to the drive current, and goes from 0 mW for $I \leq 1$ A to 730 mW at $I = 2.5$ A. When the diode current is rapidly changed as in experiments, the laser power stabilizes in a millisecond time scale. The actual light power at the sample position should be reduced by a factor of 2 owing to the presence of various optical components in the beam path (Svoboda and Block 1994). The temperature of the sample was controlled from ambient (23 °C) to 37 °C, using a system that heats up the observation dish and the objective (Bioptechs, Butler, Pa., USA). Experiments were

Table 1 Quantification of fibronectin density

Concentration (μg/ml)	Fluorescence intensity (arbitrary unit)	Fibronectin density (molecules/μm^2)
0	0	0
0.3	8 ± 2	90
1	29 ± 3	290
3	106 ± 6	860
10	300 ± 100	2860 ± 750

performed under DIC illumination, and filmed with a CCD camera (Cohu, San Diego, Calif., USA). Video images were digitized using a computer (Power MacIntosh, Apple) equipped with a frame grabber card (Scion, Frederick, Md., USA).

Cell manipulation

Cells from a 1 cm^2 culture well were detached using 0.005% trypsin-20 mM EGTA in McCoy's 5A medium lacking Ca^{2+}, resuspended in culture medium containing 20 mM Hepes, and added to the observation chamber placed on the stage of the microscope. The optical trap was first set to its maximum power, allowing the capture of one cell from the suspension (Fig. 1A). The cell was brought to the floor of the chamber by turning down the focus knob. At this point, the trap force was adjusted to a given value (called compressive force, F_{comp}) by controlling the laser power. The cell was maintained in contact with the substrate for a given time period (1, 2, 4, 8, and 16 s), by adjusting the trap center on the surface (Fig. 1B). The lower time limit (1 s) was set by manipulation speed, while the upper time (16 s) already led to maximal adhesion. In some experiments, a very brief contact duration was achieved (a fraction of a second), and is taken as the zero time point. At the end of the incubation period, the laser power was adjusted to a second value (corresponding to a given pulling force, F_{pull}), and the focus knob was quickly turned upwards (about 30 μm in 0.5 s) to detach the cell. If the cell stuck to the substrate, it was counted as adherent (Fig. 1C). If it moved along with the trap, it was counted as detached (Fig. 1D). The cell was not reused. An experiment consisted of about 10 cells for each time point, and lasted around 20 min. In some cases, 1 μg/ml cytochalasin D (Sigma), 400 μg/ml Gly-Arg-Gly-Asp-Thr-Pro (RGD) peptides (Sigma) or 20 μg/ml polyclonal goat anti-rabbit $\alpha_5\beta_1$, mouse anti-human β_1 (clone JB1a), polyclonal rabbit anti-mouse α_5 (Chemicon, Harrow, UK) or mouse anti-chick β_1 clone W1B10 (Sigma) were added to the suspension. In other manipulations, fibroblasts were maintained on the substrate for extended periods of time (up to 3 min) until Brownian motion ceased: this was assessed visually. Several observations suggest that laser tweezers caused no apparent damage to fibroblasts: (1) cells retained a regular rounded morphology when held in the trap for over 15 min; (2) cell lysis was never observed; (3) cells adhered well when kept on the substrate for several minutes; and (4) cells used for adhesive tests evenly spread on the substrate afterwards, like control cells that had not been exposed to the laser.

Vertical force calibration

To determine the force imposed by the optical trap on a cell at a given laser power, a cell was captured and placed 20 μm above the coverslip. The focus was maintained at constant position, while the whole chamber was moved downwards by 25 μm linearly with time, using a custom-made support driven by a piezoelectric translator (Physik Instrumente, Waldbronn, Germany). The time course was adjusted up and down by computer (Power Macintosh, Apple) through a digital-analog interface (LabView 5.0, National Instruments, Austin, Tex., USA). The cell escaped the trap at a critical speed V, quite reproducible and taken as bulk fluid velocity around the cell. The experiment was repeated for varying laser intensities and for different cells ($n = 12$), to take into account cell-to-cell variation. The maximal force exerted by the trap was taken as the drag on the cell, plus its weight. The drag for a sphere moving perpendicular to a wall is given by $\lambda 6\pi\eta r V$ (Happel and Brenner 1991), where η is the medium viscosity (taken as that of water, $\eta = 10^{-3}$ kg m^{-1} s^{-1}), r the cell radius ($r = 6.7 \pm 0.6$ μm), and λ a correction factor to Stokes formula; λ is a function of the ratio between the cell radius and the distance to the wall ($\lambda = 1.35$ in our experimental conditions). Cell weight was calculated from cell volume and density (1.05 g/ml), as described (Thoumine and Ott 1997). The maximal force was exponentially dependent on laser power (Fig. 2). Since the cell diameter (about 14 μm) is much larger that the laser wavelength (1.064 μm), we could use calculations in the ray optics regime, which show that the axial force exerted by a well-focused optical trap on a dielectric sphere is maximal at a vertical distance approximately equal to the radius of the captured object (Ashkin 1992); this is the location where the medium-to-cell step in refraction index occurs. Tracking the motion of cells attracted by optical tweezers showed that cells reached the greatest velocity at a distance of about 6–7 μm from the trap center, confirming that the trap force is maximal at the cell radius (at least in the x-y plane). Based on those arguments, the force exerted during compression (where the trap is focused at the cell-substrate interface) was taken equal to the maximal force. During pulling, the

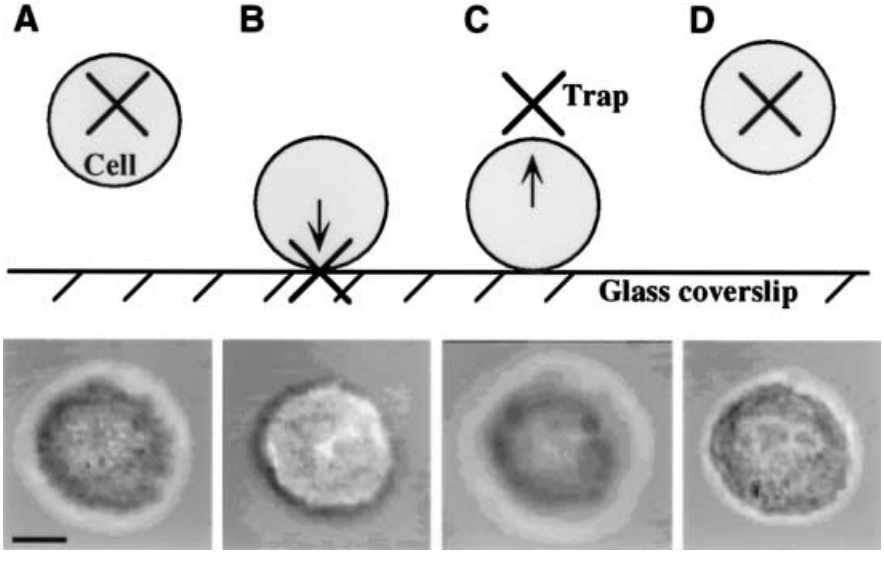

Fig. 1A–D Experimental design. (*upper panel*) side view sketches and (*lower panel*) video images of a manipulated cell. **A** A fibroblast is held above the substrate by the optical trap (*cross*); the cell is slightly out of focus, being pulled down by its own weight. **B** The trap is focused at the chamber floor, giving rise to a small reflection on the camera (*bright dot*) which helps identifying the focal point. This imposes an additional downward force on the cell. The trap is then raised by about 30 μm in 0.5 s, producing an upward force on the cell. If the cell has stuck to the substrate, it becomes out of focus **C**. If the cell has not adhered, it follows the trap **D**. *Bar*, 5 μm

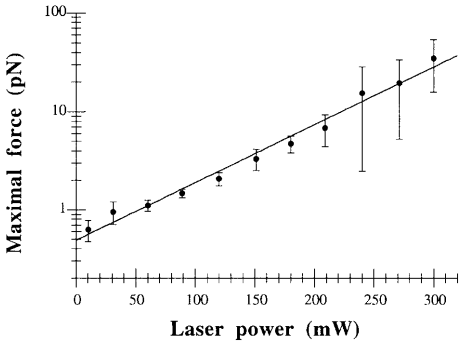

Fig. 2 Relationship between laser power and maximal trapping force. The force was determined by imposing fluid movement around the cell with increasing velocity, until the cell escaped the trap. Values represent the mean ± SD for 12 cells. The escape force at maximal power corresponded to a fluid velocity too high to be reached by our system, and was thus estimated by extrapolation of the exponential fit (*solid line*)

force applied on the cell varies with time in a non-linear fashion, reaching a maximum when the focal plane passes near the edge of the cell.

Statistics

Adhesion tests, representing about 10 cells for each time point, were repeated three times (on different days), for each condition (ligand density, temperature, compressive and pulling force). The cumulated fraction of adherent cells was computed for the three sets of 10 trials, the three sets of 20 trials, and the one set of 30 trials. The overall adhesion probability is expressed as the mean ± SD of these seven data sets. For a particular series of conditions (ligand density = 290 molecules/μm^2, compressive force = 13 pN, pulling force = 64 pN, temperature = 23 °C), 120 trials were available. The cumulated adhesion probability computed from these data was very stable for each contact duration (e.g. the value after only 10 trials was within several percent of the final value), showing that 30 cells was a reliable sampling number. To compare different conditions, unpaired *t*-tests were carried out, significance being set at the 95% level.

Theoretical analysis

At time zero, the cell is placed in contact with the fibronectin-coated substrate. Adhesion is considered to rely on the specific interaction between fibronectin and its membrane receptors on the cell surface (Fig. 3). Fibroblasts actually express several integrins that can function as fibronectin receptors (in particular $\alpha_3\beta_1$, $\alpha_4\beta_1$, $\alpha_5\beta_1$, and $\alpha_v\beta_1$), $\alpha_5\beta_1$ being the most abundant and having the highest affinity (Akiyama et al. 1990). We focus on the population of R receptors capable of binding. Each receptor can be either free

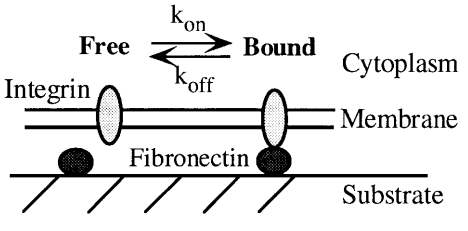

Fig. 3 Schematic drawing of the adhesive contact

(state 0) of bound to a fibronectin molecule (state 1). Let $p_0(t)$ and $p_1(t)$, respectively, denote the probabilities for a given receptor to be in either state 0 or 1 at time t. Taking the adhesive interaction as a first-order reversible chemical reaction driven by two kinetic parameters, a rate of association k_{on} and a rate of dissociation k_{off} (both in s^{-1}), one can write the following equations:

$$dp_0/dt = -k_{on}p_0 + k_{off}p_1 \quad (1)$$

$$p_1(t) = 1 - p_0(t) \quad (2)$$

The 1:1 stochiometry of binding is well known from biochemical studies (Ruoslahti 1988). We assume that the number of fibronectin molecules available for binding is in excess and we take it as constant; thus, ligand density does not appear in the equations but implicitely affects the coefficient k_{on}. With the initial conditions $p_0(0) = 1$ and $p_1(0) = 0$ (no bond), the solution of the system (1–2) is:

$$p_1(t) = k_{on}\{1 - \exp[-(k_{on} + k_{off})t]\}/(k_{on} + k_{off}) \quad (3)$$

Assuming that each receptor behaves independently, the probability $P_C(t)$ that C receptors ($C = 0$ to R) are bound at time t can be described by a binomial distribution (Chesla et al. 1998), that is:

$$P_C(t) = \binom{R}{C}(p_1(t))^C(1 - p_1(t))^{R-C} \quad (4)$$

The mean and variance of the distribution are respectively equal to $Rp_1(t)$ and $Rp_1(t)[1 - p_1(t)]$, consistently with a formulation based on small system kinetics (Cozens-Roberts et al. 1990; Piper et al. 1998). Equation (4) also agrees with a direct numerical integration of Master's equations (Kaplanski et al. 1993). The probability for a cell of being attached is then:

$$P_a(t) = \sum_{C=n}^{R} P_C(t) = 1 - \sum_{C=0}^{n-1} P_C(t) \quad (5)$$

where the integer n denotes the number of bonds necessary for adhesion. As an example, one obtains for $n = 1$: $P_a(t) = 1 - [1 - p_1(t)]^R$. Equation (5) predicts that the fraction of adherent cells increases from 0 to a plateau, with a time course and equilibrium value depending on k_{on}, k_{off}, and n (not shown). For n being maintained constant (1, 2, or 3), the rates k_{on} and k_{off} were determined by a least squares fit of the theoretical curves to the experimental data of adhesion probability versus contact duration, using commercially available software (Kaleidagraph, Abelbeck). Parameters were obtained for the different sets of data, and averaged.

Results

Overall behavior

We used optical tweezers to maintain fibroblasts on fibronectin-coated glass, adjusting the compressive force on the cell (Fig. 1A, B). After given time periods, a controlled pulling force was applied to detach the cell. We observed an all-or-none behavior: either the cell stayed stuck, or it moved along with the tweezers (Fig. 1C, D). This frank behavior enabled us to compute the adhesion probability (or fraction of adherent cells) versus time, under different conditions (fibronectin surface density, compressive and pulling forces, and temperature), changing one variable at a time. In very few cases (three out of a total of about 4500 tests) we noted a sort of elastic resistance when the tensile force

was applied, followed by yield. This was probably due to the formation of lipid tethers. Such behavior is typical of other cell types, i.e. neurons (Dai and Sheetz 1995) and leukocytes (Shao and Hochmuth 1996), but seems to be marginal in the case of fibroblasts in this force-velocity range. Decreasing the pulling velocity by 10 (to about 6 μm/s) or treating cells with cytochalasin to weaken attachment of the membrane to the actin cortex did not increase the occurrence of tethers (not shown). Adhesion times were kept very short ($1 \le t \le 16$ s) to reveal the formation of initial bonds. Two observations suggested that the number of bonds was indeed quite low at this time scale: (1) when maintained on the surface, cells exhibited significant Brownian motion, which decreased to zero in 71 ± 30 s ($n = 8$ cells), presumably corresponding to a progressive accumulation of bonds (Pierres et al. 1995a); and (2) when the pulling force was applied, adherent cells often rotated around the optical axis, as if being held only at one pivot point.

Effect of pulling force

To obtain more quantitative information about bond number, we varied the pulling force, F_{pull} (between 0 and 64 pN), expecting a detectable change in adhesion probability when the force became sufficient to break one bond. Indeed, the adhesion curves for pulling forces $F_{pull} \le 13$ pN on one hand, and those for forces $F_{pull} \ge 28$ pN on the other hand, were almost coincident, so we pooled and averaged the data for these two sets of forces. The adhesion probability for $F_{pull} \le 13$ pN was above the one for $F_{pull} \ge 28$ pN at all time points (the difference was significant at $t = 1$ and 8 s), suggesting that higher forces enhanced cell detachment (Fig. 4). Moreover, the curve obtained for lower forces was best fit by the mathematical expression characterizing adhesion by the presence of at least one bond. In contrast, the curve for higher forces showed an inflection point and was best fit by the theoretical expression describing adhesion by the existence of at least two bonds. This transition suggested that the strength of a bond was between 13 and 28 pN. Variability in both bond strength and trapping force precluded better sensitivity in this estimate. Fitting the data with the respective equations gave the kinetic rates k_{on} and k_{off}, which were used to compute the probability distributions at different times (Fig. 5A–C). Also shown is the predicted average number of bonds (Fig. 5D), which increases exponentially and reaches about 7 at a contact duration of 16 s, under these conditions. Finally, the association rate found from the fits was inversely dependent on the receptor number R, i.e. the product $k_{on}R$ was constant for a given adhesion curve. Thus, we defined a more stable parameter, i.e. the overall cell association rate constant $k_+ = k_{on}R$. In contrast, k_{off} was independent of R.

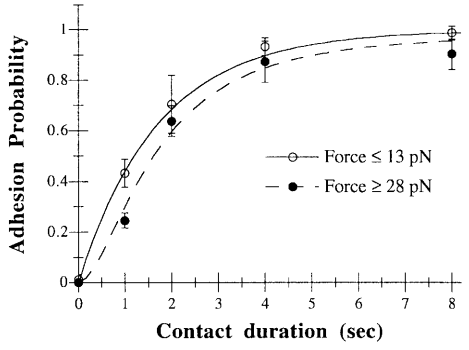

Fig. 4 Effect of pulling force on adhesion. Cells were placed in contact with the fibronectin-coated coverslip (density 290 molecules/μm^2) at a fixed compressive force of 13 pN and at 23 °C. After a given time period, the cells were pulled upwards with a force of 2.5, 5.6, 13, 28, or 64 pN. Forces below 13 pN and above 28 pN, respectively, were pooled and averaged. Chi-square (χ^2) tests were performed to assess the goodness of the fits. For $F_{pull} \le 13$ pN, these gave $\chi^2 = 0.61$ for $n = 1$ versus $\chi^2 = 1.56$ for $n = 2$ and $\chi^2 = 118$ for $n = 3$, while for $F_{pull} \ge 28$ pN, $\chi^2 = 15.3$ for $n = 1$, $\chi^2 = 5.0$ for $n = 2$, and $\chi^2 = 40$ for $n = 3$ (values below 9.5 are significant). Data for lower forces were thus fit by Eq. (5) with $n = 1$ (*solid curve*), giving $k_{on} = 1.64 \times 10^{-6}$ s^{-1} and $k_{off} = 0.09$ s^{-1} (taking $R = 5 \times 10^5$), whereas the data for upper forces were fit by Eq. (5) with $n = 2$ (*dashed curve*), giving $k_{on} = 2.50 \times 10^{-6}$ s^{-1} and $k_{off} = 0.21$ s^{-1}. Note that higher forces decrease adhesion and exhibit an inflexion point at about 0.5 s. The plot is cut at $t = 8$ s to better illustrate the difference; data points at $t = 16$ s are respectively $P_a = 0.99 \pm 0.03$ ($F_{pull} \le 13$ pN) and $P_a = 0.98 \pm 0.03$ ($F_{pull} \ge 28$ pN)

Effect of fibronectin density

The adhesion probability increased with fibronectin density, reaching 100% in several seconds (Fig. 6A). RGD peptides reduced adhesion probability by 10–100%, depending on time (the difference was significant at all time points), suggesting an integrin molecule was involved in binding. The parameters k_+ and k_{off} were calculated from these adhesion curves: k_+ increased noticeably with fibronectin density, whereas k_{off} did not show a consistent trend (Fig. 6B). Since bond formation involves both the diffusion of a receptor to the vicinity of an immobilized ligand (rate k_{diff}), and the chemical reaction itself (rate k_{reac}), the overall association rate constant may be written as (Bell 1978):

$$k_+ = (1/k_{diff} + 1/k_{reac})^{-1} \quad (6)$$

Theory further shows that (Lauffenburger and Linderman 1993; Schmidt et al. 1994):

$$k_{diff} = 2\pi D R_T / [A_T \ln(b/s)] \quad (7)$$

where D is the diffusion coefficient of receptors in the plane of the membrane, i.e. 0.01–0.1 μm^2/s for the β_1 integrin subunit (Duband et al. 1988; Felsenfeld et al. 1996; Choquet et al. 1997), $R_T = 1$–5×10^5, the total number of fibronectin receptors on a fibroblast surface (Akiyama and Yamada 1985; Codogno et al. 1987), $A_T = 1500$ μm^2, the total cell surface area including membrane wrinkles (Thoumine et al. 1999), b is one half the mean distance between ligand molecules, i.e.

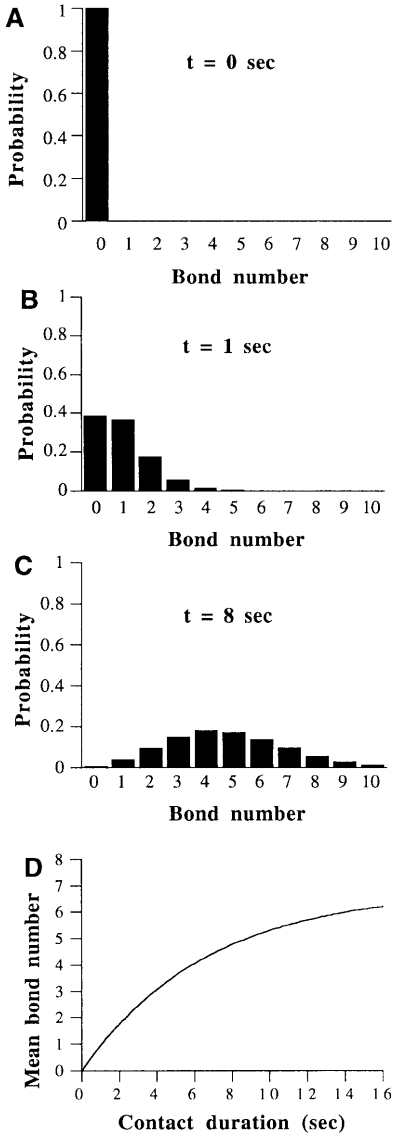

Fig. 5A–D Bond distribution over time. The binomial distribution (Eq. 4) is shown at three different contact durations, i.e. 0 s (**A**), 1 s (**B**), and 8 s (**C**). The average bond number is shown in (**D**). Parameters were intermediary between those determined from Fig. 4 ($k_{on} = 2.05 \times 10^{-6}$ s^{-1}; $k_{off} = 0.15$ s^{-1})

$b = 1/(\pi N_L)^{1/2}$ where N_L is the ligand density, and s the encounter radius (theoretically in the range of 1–10 nm). By replacing, one obtains:

$$k_+ = [1/k_{reac} - (A_T/2\pi D R_T)\ln(s\sqrt{\pi N_L})]^{-1} \quad (8)$$

A fit of the k_+ data with this expression gives the lumped parameter $A_T/4\pi D R_T = 0.38$ s, and the relation $1/k_{reac} = 3.70 + 0.76\ln(s\sqrt{\pi})$ (seconds), with s in μm. Since $k_{reac} \geq 0$, this sets a lower limit $s = 4$ nm.

Effect of temperature

Increasing the temperature (from 23 to 37 °C) significantly raised the adhesion probability (Fig. 7A) as well

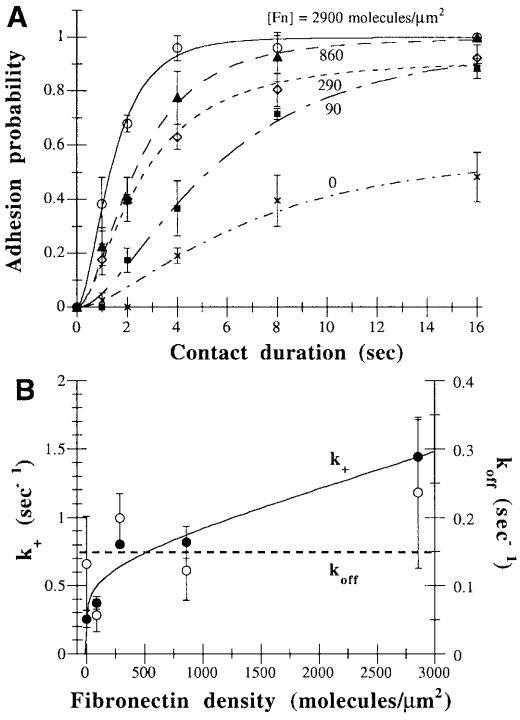

Fig. 6A, B Effect of fibronectin density on adhesion. The fibronectin density was varied between 0 and 2900 molecules/μm^2, at constant compressive force (13 pN), traction force (64 pN), and temperature (23 °C). Since F_{pull} is enough to break a bond, the theoretical expression (*solid and dashed curves*) corresponds to Eq. (5) with $n = 2$ bonds. The parameters k_+ and k_{off} found from the fits are shown in **B** versus fibronectin density (*filled and empty circles*, *respectively*). The *solid curve* represents the least-squares fit $k_+ = [3.7–0.38\ ln(N_L)]^{-1}$, as described by Eq. (8), with regression coefficient $r = 0.94$. The *dashed line* is the average of the k_{off} data (0.15 ± 0.07 s^{-1}). Adhesion data in the presence of RGD peptides was fitted with the coefficients $k_+ = 0.45 \pm 0.10$ s^{-1} and $k_{off} = 0.07 \pm 0.04$ s^{-1}, to be compared with control data for $N_L = 860$ molecules/μm^2 in **B**

as the parameters k_+ and k_{off} (Fig. 7B). The rates of a chemical reaction should be inversely proportional to the exponential of the ratio $E_a/k_B T$, where E_a is the activation energy of the chemical reaction (supposing a simple activated process), k_B is Boltzmann's constant, and T the absolute temperature (K). Indeed, the relationship between each rate constant and $1/T$ was well fit by a decreasing exponential function:

$$k = k_0 \exp(-E_a/k_B T) \quad (9)$$

where k is either k_+ or k_{off}, and the coefficient k^0 represents the corresponding parameter at infinite temperature. E_a computed from the k_+ and k_{off} data was respectively 25.3 and $16.6 \times k_B T_0$ (the thermal energy at $T_0 = 300$ K, i.e. 4.1×10^{-21} J).

Effect of compression

The higher the compressive force exerted on the cell during the contact period (from 0 to 64 pN), the larger the adhesion probability (Fig. 8A). The association rate

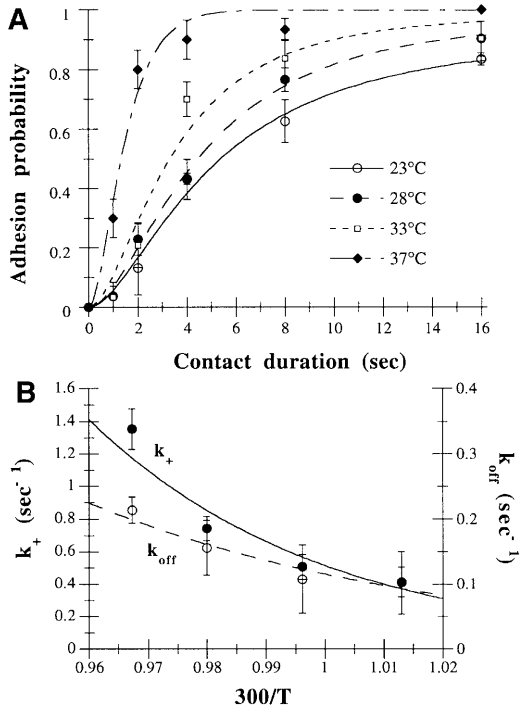

Fig. 7A, B Effect of temperature on adhesion. The temperature was varied between 23 and 37 °C, at constant fibronectin density (290 molecules/μm^2), compressive force (13 pN), and traction force (64 pN). **A** The adhesion probability was fit by Eq. (5), with $n = 2$, giving the rate constants k_+ and k_{off}. These parameters are plotted in **B** versus the ratio $300/T$, where T is the absolute temperature (K). The *solid* and *dashed curves* are exponential fits (Eq. 9) through the data ($r = 0.96$)

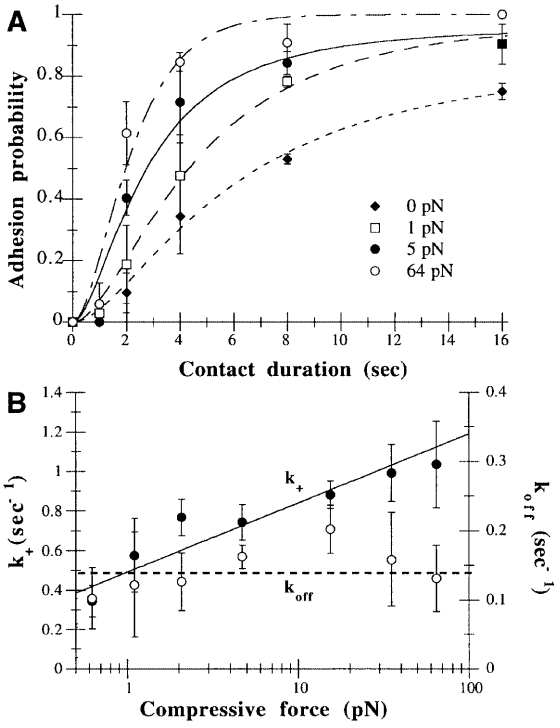

Fig. 8A, B Effect of compressive force on adhesion. **A** Compression was varied between 0 and 64 pN, at constant fibronectin density (290 molecules/μm^2), traction force (64 pN), and temperature (23 °C). The plain curves are fits of Eq. (5) with $n = 2$, which yield the two parameters k_+ and k_{off}, plotted in **B** versus the compressive force on the cell, in a logarithmic scale. The *solid line* represents the least-squares fit $k_+ = 0.49 + 0.15 \ln(F_{comp})$, with F_{comp} in pN ($r = 0.96$). The *dashed line* is the mean of the k_{off} data (0.14 ± 0.05 s^{-1})

k_+ was found to increase with compression in a logarithmic manner, whereas k_{off} remained fairly constant (Fig. 8B). It was possible that the effect of compression was actually due to local heating or photoactivation at the adhesive site, generated by the laser. The temperature increase was estimated to be 1.7 °C per 100 mW output power in an optical trap set-up similar to ours (Kuo 1998). Thus, we expect the maximal output power of about 320 mW on the sample to correspond to 5.4 °C above room temperature (i.e. 28.4 °C). This is still in the physiological range and should not cause as much an increase in adhesion if due to temperature alone (see previous paragraph). To further check for temperature effects, we carried out experiments in which the trap was placed about 15 μm above the substrate (the position of equilibrium between laser force and cellular weight), so that no compression was applied on the cell, while the laser power was maintained near its maximum (supposedly heating the sample). Adhesion in this case ($k_+ = 0.27$ s^{-1} and $k_{off} = 0.15$ s^{-1}), was similar to the situation where the laser power was zero (respectively $k_+ = 0.34$ s^{-1} and $k_{off} = 0.10$ s^{-1}), suggesting that the temperature difference between the two conditions, if any, was too small to affect adhesion. Effects other than local heating, e.g. photodamage of adhesive proteins or membrane lipids, would presumably cause a decrease in adhesion with increasing laser power, the contrary of what was observed. Thus, the increase in adhesion probability with laser power could safely be attributed to the compressive force exerted on the cell during contact.

Discussion

Overview of the approach

We reported here a sensitive method to probe the adhesion of living cells, based on optical tweezers, which allowed control of important physicochemical variables (duration of contact, compressive and tensile forces, temperature, ligand density). It is inspired by experiments where ligand-coated microspheres are placed on the surface of fibroblasts (Schmidt et al. 1993; Choquet et al. 1997) or neurons (Dai and Sheetz 1995), in order to probe membrane-cytoskeleton interaction. The time scales of adhesion were similar to ours, i.e. several seconds for comparable densities of ligand adsorbed on the microspheres (Choquet et al. 1997). Our method is simple and fast (i.e. one can test about 50 cells in 20 min), allowing a reliable statistical analysis, which was manifest in the smoothness and reproducibility of the adhesion curves. Moreover, the technique can easily

be adapted to the study of other adhesive systems (e.g. involving different cell types and extracellular ligands), and not only cell-matrix interactions. For example, by letting a cell monolayer cover the substrate, one may also probe cell-cell adhesion. It should also be feasible to visualize the contact zone by fluorescence or reflection microscopy and correlate such observations to the adhesion data. Finally, since 3T3 fibroblasts can be transfected with genes of mutated receptors (Felsenfeld et al. 1996; Choquet et al. 1997), this approach may be further used to study the correlation between the structure of an adhesion receptor and its physical properties.

Adhesion tests were interpreted using a probabilistic analysis, based on previous work (Cozens-Roberts et al. 1990; Chesla et al. 1998; Piper et al. 1998) which predicted the bond distribution at each time point. For example, the average number of adhesive bonds at a 16 s contact duration is close to $0.9\,k_+/k_{\mathrm{off}}$ (see Eq. 3) and lies between 3 and 9, depending on experimental conditions. Given few limiting hypotheses (e.g. first-order reversible reaction, independent behavior of receptors), the model provided analytical expressions which fit the data quite well and allowed simple extraction of kinetic parameters. Given fibronectin densities of 100–3000 molecules/μm^2 and contact areas in the range of 0.1–1 μm^2 (see next paragraph), the average number of fibronectin molecules in the contact zone (10–3000) is much higher than the number of bonds formed (just a few); thus, it is a good approximation to neglect ligand depletion here. More complex types of interactions, e.g. involving an intermediate state binding (Pierres et al. 1995b), a different stochiometry (Chesla et al. 1998), or receptor coupling to the cytoskeleton (Thoumine and Meister 2000) may be treated similarly. Changes in the rates of bond association and dissociation versus the experimental conditions (temperature, tensile and compressive forces) give insight into the intrinsic physical properties of the interaction between fibronectin and its membrane receptor.

Bond formation

The overall association rate k_+ was in the range of 0.3–1.4 s^{-1}, similar to values reported for the E-selectin-dependent adhesion of granulocytes to the endothelium (Kaplanski et al. 1993). k_+ increased with fibronectin density in a non-linear manner: this was interpreted as association being made of two steps, namely diffusion and reaction. Fitting the data with the theory gave the lumped parameter $A_T/4\pi DR_T = 0.38$ s, which falls in the right range for realistic values of the parameters, and the reaction rate k_{reac} as a function of the encounter radius, s. Given these relations, we can estimate orders of magnitude for the kinetic rates k_{diff} and k_{reac}. For example, at low ligand density (e.g. $N_L = 100$ μm^{-2}) and for the lower value $s = 5$ nm, one obtains $k_{\mathrm{diff}} = 0.55$ s^{-1} and $k_{\mathrm{reac}} = 9.2$ s^{-1} (giving $k_+ = 0.52$ s^{-1}), in which case the fibronectin-receptor association is diffusion limited. At higher ligand density (e.g. $N_L = 3000$ μm^{-2}) and for the upper value $s = 10$ nm, one obtains $k_{\mathrm{diff}} = 45$ s^{-1} and $k_{\mathrm{reac}} = 1.6$ s^{-1} (giving $k_+ = 1.55$ s^{-1}), falling in the reaction-limited regime. For intermediate values of these parameters, both steps contribute to bond formation.

k_+ increased by about three-fold with the compressive force applied on the cell (in the range of 0.5–64 pN), independently of temperature effects. This is comparable to granulocytes interacting with endothelial cells: their association rate is 0.04 s^{-1} when the cells are freely rolling, and increases by 10-fold after initial contact (Kaplanski et al. 1993). In that situation, leukocytes are indeed pulled upstream by the first bond, and compressed downstream because of torque effects due to the velocity gradient (Hammer and Lauffenburger 1987; Chang and Hammer 1996). As a first approximation, k_+ should be proportional to the contact area A_c between the cell and the substrate, i.e. $k_+ = k_+^{\max} A_c/A_T$, where A_T is the total cell surface area and $k_+^{\max}$ the maximal association rate (if all the area was available for binding). Considering the fibroblast as a fluid drop bounded by a cortex under a persistent tension $T = 3 \times 10^{-4}$ N/m (Thoumine et al. 1999), a simple mechanical equilibrium gives an apparent contact area (neglecting surface roughness) $A_c = R_0 F_{\mathrm{comp}}/2T$, where F_{comp} is the compressive force and R_0 the cell radius (about 8 μm). Thus one expects k_+ to be proportional to the force on the cell, but the actual dependence is logarithmic. One explanation for this discrepancy is that because of membrane wrinkles, the actual contact surface is not a mere disc and the contact area does not increase linearly with compression. Repulsion from the glycocalyx may also play a role in this phenomenon.

The intrinsic association rate per receptor (k_{on}) was found inversely proportional to the number of available receptors chosen in the model. This is because receptors compete with one another for binding (Lauffenburger and Linderman 1993). For example, if we consider that all receptors on the cell surface are capable of binding, i.e. $R = R_T = 5 \times 10^5$, then k_{on} is on the order of 10^{-6} s^{-1}. However, because of membrane barriers to diffusion (Sheetz 1993), probably only the receptors in the contact zone can interact (e.g. it would take a time $\pi^2 R_0^2/2D$ = about 2 h for a receptor to diffuse from top to bottom of the cell, which is much larger than the time scale of adhesion tests). Taking a contact area of 0.2 μm^2 (value for a compressive force $F_{\mathrm{comp}} = 15$ pN), then $R = 50$ and k_{on} is around 10^{-2} s^{-1}. Finally, depolymerizing actin by treating cells with cytochalasin decreased k_+ by a factor of 2 (not shown), suggesting that interaction with an intact actin network on the cytoplasmic side facilitates receptor binding to fibronectin, possibly through a two-state conformational change of the integrin (Felsenfeld et al. 1996; Thoumine and Meister 2000).

Bond strength and energy

Once a bond is formed, cell-substrate detachment upon pulling may involve several mechanisms (Evans et al.

1991): (1) bond breakage; (2) receptor extraction; (3) membrane-cortex separation; and (4) detachment of fibronectin from the substrate. Membrane separation is unlikely since we did not observe tether formation. The fourth possibility can also be ruled out because fibronectin adsorbs very strongly to glass (Haas and Culp 1982). We are left with the two first mechanisms, which are difficult to distinguish with respect to force amplitude. Indeed, on the one hand, breakage of bonds between typical biological molecules i.e. actin to α-actinin (Miyata et al. 1996) or two antibodies bound on red blood cells (Tha et al. 1986), involve forces of 18 pN and 10 pN, respectively, similar to that reported here (between 13 and 28 pN). On the other hand, the forces holding proteins in the plasma membrane are also on the order of 20 pN, as assessed theoretically (Bell 1978) and experimentally (Evans et al. 1991). One way to distinguish between bond breakage and receptor extraction is to keep testing the same cell throughout a time series until it stays adhered, then repeat the experiment with other cells until enough data are gathered. If receptor extraction occurs, then one should observe a decrease in adhesion probability versus control conditions where each cell is tested only once, indicating irreversibility of binding (Chesla et al. 1998). Moreover, the difference should be larger at high pulling forces, when one can detach the cell. However, the curves obtained in such experiments both at low and high pulling forces were similar to control (not shown), suggesting that in our experiments, bond failure is the dominant mechanism. Both k_+ and k_{off} increased about three-fold with temperature between 23 and 37 °C. This is likely due to facilitated passage through activation barriers in both directions of the reaction, and/or an increase in membrane fluidity resulting in faster receptor diffusion. An activation energy of about 20 times the thermal energy at 300 K was deduced from the relationship between the reaction rate constants and the temperature, which reflects the energy well of the fibronectin-receptor interaction. This value is in agreement with the free energy minimum of protein G-IgG bonds, i.e. 35 $k_B T_0$ (Kwong et al. 1996).

Bond rupture

The rate of dissociation between adsorbed fibronectin and its receptor, k_{off}, was in the range of 0.05–0.3 s^{-1}, and rather independent of ligand density and compression. This is faster than the dissociation rate of soluble fibronectin from epithelial cells in suspension, namely 0.01 s^{-1} (Akiyama and Yamada 1985; Lauffenburger and Linderman 1993). The fact that fibronectin is coupled to a substrate probably induces mechanical constraints on the molecule, making it more likely to dissociate. The discrepancy may also come from differences in cell types and fibronectin species. For comparison, k_{off} is in the same range as that reported for the interaction between collagen or laminin and $\alpha_2\beta_1$ integrin, i.e. 0.06 s^{-1} under non-activating conditions (Masson-Gadais et al. 1999), but lower than that between a selectin and its carbohydrate ligand in situations of leukocyte rolling, i.e. 0.5–3 s^{-1} (Kaplanski et al. 1993; Alon et al. 1995), between integrins and the underlying cytoskeleton at the dorsal surface of fibroblast lamellae, i.e. 3 s^{-1} (Schmidt et al. 1994), or between CD2 and CD28 molecules mediating lymphocyte adhesion, i.e. above 8 s^{-1} (Pierres et al. 1996). Supposedly, those last three biological situations require very dynamic interactions, whereas in the case of fibroblasts interacting with a fibronectin matrix, a lower dissociation rate promotes stabilization of newly formed adhesion sites. Integrins and selectins are actually expected to display different binding kinetics, in view of their complementary roles in leucocyte-endothelial adhesion (Springer 1994).

Since the pulling force is likely to increase k_{off} in an exponential fashion (Bell 1978; Cozens-Roberts et al. 1990), the bond strength (20 pN) may also be considered as the force required to reduce the bond lifetime ($1/k_{off}$) until it becomes negligible with respect to the pulling time (approximately 0.5 s). In other words, the probability of bond dissociation (viewed as a stochastic event) is high under such force in the time scale of the experiment. We identified a narrow range of forces (13–28 pN) characterizing the rupture of fibronectin-integrin linkages, in agreement with sharp strength distributions obtained for single avidin-biotin bonds (Merkel et al. 1999). Furthermore, a theoretical analysis of bond failure showing that the probability to quickly break two or three bonds is much lower than that to break a single bond (Evans et al. 1991) supports our finding that forces of 28–64 pN break only one ligand-receptor bond. However, it should be kept in mind that the detachment force presumably increases with the rate of pulling (Merkel et al. 1999); here, the loading rate was in the range of 5–100 pN/s. When a bond breaks during pulling, it probably does so when the force reaches its maximum, i.e. when the laser trap passes near the upper edge of the cell. The pulling time was kept short compared to the contact time, so that the kinetic parameters reflected the conditions imposed during adhesion, in particular compression. However, this concern is not so critical since decreasing the pulling velocity by a factor of 10 did not change the adhesion probability (not shown).

Limitations

One drawback is that we did not achieve entire specificity of the receptor-ligand interaction, apparent in the fact that some binding was still present at zero fibronectin concentration (Fig. 6A). The best agent we found against non-specific adhesion was bovine serum, while albumin had little blocking effect (not shown). The use of 10% serum may introduce artifacts, e.g. soluble fibronectin may compete with substrate binding sites, and

adsorption of other proteins such as vitronectin to the glass coverslip may occur (although this phenomenon should be minor at short time scales). On the other hand, the biophysical parameters should be relevant to most studies of fibroblast locomotion which are usually done in serum-containing medium. Although specific adhesion of fibroblasts to fibronectin was significantly reduced by RGD peptides, we were also unable to identify precisely which receptor was involved in fibronectin recognition. It is possible that several receptors, not only the most common $\alpha_5\beta_1$ integrin, were implicated in binding fibronectin, in which case the kinetic coefficients would represent an average behavior. The antibodies against α_5 or β_1 integrin subunits did not significantly alter adhesion. Supposedly, these did not have any particular activating or inhibiting role, as has been reported for some antibodies to $\alpha_2\beta_1$ integrins (Masson-Gadais et al. 1999). The detachment protocol should not damage the fibronectin receptors, which are sensitive to trypsin only at 50-fold higher doses (i.e. 0.25%) than the ones used here (Akiyama and Yamada 1985).

There are also some uncertainties associated with force measurements. Calibration was done with Stokes drag on fibroblasts about 20 μm above the surface. This is probably a good approximation when one pulls on the cell after contact by raising the trap away from the coverslip; thus, the estimate of bond strength should be fairly accurate. Furthermore, vertical forces are similar to those determined for 2–11 μm latex particles in the lower range of laser power (Misawa et al. 1991) and, in the higher range, with forces necessary to aspirate the same cells in a thin micropipet coming from the top (not shown). However, during compression, the laser trap is focused on the surface, and there may be subtle optical effects (scattering, interference) modifying its behavior. Thus, the values of compressive force may only be good within a factor of 2 or so, although this does not affect the qualitative picture that bond formation increases with compression. Finally, we cannot rule out that some local photoactivation is taking place during contact, enhancing the interaction. Despite these drawbacks that can hopefully be solved in future studies, we believe that we demonstrated the potential of our method to accurately quantify cell adhesion.

Conclusion

We reported here short-term adhesion tests using optical tweezers which, coupled to a probabilistic model of receptor-ligand kinetics, yielded information about the number, strength, and reaction rates of bonds between fibroblasts and fibronectin. This may serve to better understand the locomotion of fibroblasts and their interaction with the extracellular matrix in the connective tissue. This approach also opens the way to a systematic comparison of the biophysical properties of the different types of receptor-ligand interactions. Such knowledge is important for a better understanding of how adhesive interactions are controlled in time and space, leading, for example, to coordinated immune responses or tissue morphogenesis.

Acknowledgements This work was supported by funds from our institute. The authors thank D. Choquet, P. Cluzel, and T.M. Quinn for fruitful discussions, A. Ott for critical reading of the manuscript, and people at the chemistry department for letting us use their spectrophotometer.

References

Akiyama SK, Yamada SS (1985) The interaction of plasma fibronectin with fibroblastic cells in suspension. J Biol Chem 260: 4492–4500

Akiyama SK, Nagata K, Yamada KM (1990) Cell surface receptors for extracellular matrix components. Biochim Biophys Acta 1031: 91–110

Alon R, Hammer DA, Springer TA (1995) Lifetime of the P-selectin-carbohydrate bond and its response to tensile force in a hydrodynamic flow. Nature 374: 539–542

Ashkin A (1992) Forces of a single-beam gradient laser trap on a dielectric sphere in the ray optics regime. Biophys J 61: 569–582

Ashkin A, Dziedzic JM, Yamane T (1987) Optical trapping and manipulation of single cells using infrared laser beams. Nature 330: 769–771

Bell GI (1978) Models for the specific adhesion of cells to cells. A theoretical framework for adhesion mediated by reversible bonds between cell surface molecules. Science 200: 618–627

Chang KC, Hammer DA (1996) Influence of direction and type of applied force on the detachment of macromolecularly-bound particles from surfaces. Langmuir 12: 2271–2282

Chesla SE, Selvaraj P, Zhu C (1998) Measuring two-dimensional receptor-ligand binding kinetics by micropipette. Biophys J 75: 1553–1572

Choquet D, Felsenfeld DP, Sheetz MP (1997) Extracellular matrix rigidity causes strengthening of integrin-cytoskeletal linkages. Cell 88: 39–48

Codogno P, Doyennette-Moyne MA, Aubery M (1987) Evidence for a dual mechanism of chick embryo fibroblast adhesion on fibronectin and laminin substrata. Exp Cell Res 169: 478–489

Cozens-Roberts C, Lauffenburger DA, Quinn JA (1990) Receptor-mediated cell attachment and detachment kinetics. I. Probabilistic model and analysis. Biophys J 58: 841–856

Dai J, Sheetz MP (1995) Mechanical properties of neuronal growth cone membranes studied by tether formation with laser optical tweezers. Biophys J 68: 988–996

Dembo M, Torney DC, Saxman K, Hammer D (1988) The reaction-limited kinetics of membrane-to-surface adhesion and detachment. Proc R Soc Lond B 234: 55–83

Duband JL, Nuckolls GH, Ishihara A, Hasegawa T, Yamada KM, Thiery JP, Jacobson K (1988) Fibronectin receptor exhibits high lateral motility in embryonic locomoting cells but is immobile in focal contacts and fibrillar streaks in stationary cells. J Cell Biol 107: 1385–1396

Evans E, Ritchie K (1997) Dynamic strength of molecular adhesion bonds. Biophys J 72: 1541–1555

Evans E, Berk D, Leung A (1991) Detachment of agglutinin-bonded red blood cells. I. Forces to rupture molecular-point attachments. Biophys J 59: 838–848

Evans E, Ritchie K, Merkel R (1995) Sensitive force technique to probe molecular adhesion and structural linkages at biological interfaces. Biophys J 68: 2580–2587

Felsenfeld DP, Choquet D, Sheetz MP (1996) Ligand binding regulates the directed movement of $\beta 1$ integrins on fibroblasts. Nature 383: 438–440

Haas R, Culp LA (1982) Properties and fate of plasma fibronectin bound to the tissue culture substratum. J Cell Physiol 113: 289–297

Hammer DA, Lauffenburger DA (1987) A dynamical model for receptor-mediated cell adhesion to surfaces. Biophys J 52: 475–487

Happel J, Brenner H (1991) Low Reynolds number hydrodynamics. Kluwer, Dordrecht, pp 329–331

Hinterdorfer P, Baumgartner W, Gruber HJ, Schilcher K, Schindler H (1996) Detection and localization of individual antibody-antigen recognition events by atomic force microscopy. Proc Natl Acad Sci USA 93: 3477–3481

Huttenlocher A, Sandborg RR, Horwitz AF (1995) Adhesion in cell migration. Curr Opin Cell Biol 7: 697–706

Ingber DE (1990) Fibronectin controls capillary endothelial cell growth by modulating cell shape. Proc Natl Acad Sci USA 87: 3579–3583

Kaplanski G, Farnarier C, Tissot O, Pierres A, Benoliel AM, Alessi MC, Kaplanski S, Bongrand P (1993) Granulocyte-endothelium initial adhesion: analysis of transient binding events mediated by E-selectin in a laminar shear flow. Biophys J 64: 1922–1933

Kuo SC (1998) A simple assay for local heating by optical tweezers. Methods Cell Biol 55: 43–45

Kwong D, Tees DFJ, Goldsmith HL (1996) Kinetics and locus of failure of receptor-ligand-mediated adhesion between latex spheres. II. Protein-protein bond. Biophys J 71: 1115–1122

Lauffenburger DA, Horwitz AF (1996) Cell migration: a physically integrated molecular process. Cell 84: 359–369

Lauffenburger DA, Linderman JJ (1993) Receptors: models for binding, trafficking, and signaling. Oxford University Press, New York

Lotz MM, Burdsal CA, Erickson HP, McClay DR (1989) Cell adhesion to fibronectin and tenascin: quantitative measurements of initial binding and subsequent strengthening response. J Cell Biol 109: 1795–1805

Masson-Gadais B, Pierres A, Benoliel A-M, Bongrand P, Lissitzky J-C (1999) Integrin α and β subunit contribution to the kinetic properties of $\alpha_2\beta_1$ collagen receptors on human keratinocytes analyzed under hydrodynamic conditions. J Cell Sci 112: 2335–2345

Merkel R, Nassoy P, Leung A, Ritchie K, Evans E (1999) Energy landscapes of receptor-ligand bonds explored with dynamic force spectroscopy. Nature 397: 50–53

Misawa H, Koshioka M, Sasaki K, Kitamura N, Masuhara H (1991) Three-dimensional optical trapping and laser ablation of a single polymer latex particle in water. J Appl Phys 70: 3829–3836

Miyata H, Yasuda R, Kinosita K (1996) Strength and lifetime of the bond between actin and skeletal muscle α-actinin studied with an optical trapping technique. Biochim Biophys Acta 1290: 83–88

Pierres A, Benoliel A-M, Bongrand P (1995a) Use of thermal fluctuations to study the length and flexibility of ligand-receptor bonds. CR Acad Sci Paris 318: 1191–1196

Pierres A, Benoliel AM, Bongrand P (1995b) Measuring the lifetime of bonds made between surface-linked molecules. J Biol Chem 270: 26586–26592

Pierres A, Benoliel AM, Bongrand P, van der Merwe PA (1996) Determination of the lifetime and force dependence of interactions of single bonds between surface-attached CD2 and CD48 adhesion molecules. Proc Natl Acad Sci USA 93: 15114–15118

Pierres A, Benoliel AM, Bongrand P, van der Merwe PA (1997) The dependence of the association rate of surface-attached adhesion molecules CD2 and CD48 on separation distance. FEBS Lett 403: 239–244

Pierres A, Benoliel AM, Bongrand P (1998a) Interactions between biological surfaces. Curr Opin Colloid Interface Sci 3: 525–533

Pierres A, Benoliel AM, Bongrand P (1998b) Studying receptor-mediated cell adhesion at the single molecule level. Cell Adhes Commun 5: 375–395

Piper JW, Swerlick RA, Zhu C (1998) Determining force dependence of two-dimensional receptor-ligand binding affinity by centrifugation. Biophys. J. 74: 492–513

Ruoslahti E (1988) Fibronectin and its receptors. Annu Rev Cell Biol 57: 375–414

Schmidt CE, Horwitz AF, Lauffenburger DA, Sheetz MP (1993) Integrin-cytoskeletal interactions in migrating fibroblasts are dynamic, asymmetric, and regulated. J Cell Biol 123: 977–991

Schmidt CE, Chen T, Lauffenburger DA (1994) Simulation of integrin-cytoskeletal interactions in migrating fibroblasts. Biophys J 67: 461–474

Shao JY, Hochmuth RM (1996) Micropipette suction technique for measuring piconewton forces of adhesion and tether formation from neutrophil membranes. Biophys J 71: 2892–2901

Sheetz MP (1993) Glycoprotein motility and dynamic domains in fluid plasma membranes. Annu Rev Biophys Biomol Struct 22: 417–431

Springer TA (1994) Traffic signals for lymphocyte recirculation and leukocyte emigration: the multistep paradigm. Cell 76: 301–314

Stout AL, Webb WW (1998) Optical force microscopy. Methods Cell Biol 55: 99–116

Svoboda K, Block SM (1994) Biological applications of optical forces. Annu Rev Biophys Biomol Struct 23: 247–285

Tha SP, Shuster J, Goldsmith HL (1986) Interaction forces between red cells agglutinated by antibody. II. Measurement of hydrodynamic force of breakup. Biophys J 50: 1117–1126

Thoumine O, Ott A (1997) Comparison of the mechanical properties of normal and transformed fibroblasts. Biorheology 34: 309–326

Thoumine O, Cardoso O, Meister JJ (1999) Changes in the mechanical properties of fibroblasts during spreading: a micromanipulation study. Eur Biophys J 28: 222–234

Thoumine O, Meister JJ (2000) A probabilistic model for ligand-cytoskeleton transmembrane adhesion: predicting the behavior of microspheres on the surface of migrating cells. J Theor Biol 204: 381–392

Wong JY, Kuhl TL, Israelachvili JN, Mullah N, Zalipsky S (1997) Direct measurement of a tethered ligand-receptor interaction potential. Science 275: 820–822